Synthesis of Discrete CHA Zeolite Nanocrystals without Organic Templates for Selective CO 2 Capture

Maxime Debost, Paul B. Klar, Nicolas Barrier, Edwin B. Clatworthy, Julien Grand, Fabien Laine, Petr Brázda, Lukas Palatinus, Nikolai Nesterenko, Philippe Boullay, et al.

COMMUNICATION

Synthesis of discrete CHA zeolite nanocrystals without organic templates for selective CO_2 capture

Maxime Debost,[a-b] Paul B. Klar,[c] Nicolas Barrier,[b] Edwin B. Clatworthy[a] Julien Grand[a-d] Fabien Laine,[b] Petr Brázda,[c] Lukas Palatinus,[c] Nikolai Nesterenko,[d] Philippe Boullay,[b] and Svetlana Mintova*[a]*

[a] Dr. M. Debost, Dr. E. B. Clatworthy, Dr. J. Grand, Dr.S.Mintova,
Normandie Université, ENSICAEN, UNICAEN, CNRS, LCS, 14000 Caen, France

[b] Dr. N. Barrier, Dr. F. Laine, Dr. P. Boullay
Normandie Université, ENSICAEN, UNICAEN, CNRS, CRISMAT, 14000 Caen, France

[c] Dr. P. B. Klar, Dr. P. Brázda, Dr. L. Palatinus
Institute of Physics of the Czech Academy of Sciences, Na Slovance 2, Prague, Czech Republic

[d] Dr. N. Nesterenko
Total Research and Technologies, Feluy, B-7181 Seneffe, Belgium

Abstract: Small-pore zeolites such as chabazite (CHA) are excellent candidates for the selective separation of CO_2, however, the current synthesis involves several steps and the use of organic structure-directing agent (OSDA), increasing their cost and energy requirements. Here we report the synthesis of small-pore zeolite crystals (aluminosilicate) with CHA-type framework structure by direct synthesis in a colloidal suspension containing a mixture of inorganic cations only (Na^+, K^+ and Cs^+). The location of CO_2 molecules in the host structure was revealed by 3D electron diffraction (3D ED). The high sorption capacity for CO_2 (3.8 mmol/g at 121 kPa), structural stability and regenerability of the discreate CHA zeolite nanocrystals is maintained for 10 consecutive cycles without any visible degradation. The CHA zeolite (Si/Al = 2) reaches an almost perfect CO_2 storage capacity (8 CO_2 per unit cell) and high selectivity (no CH_4 was adsorbed).

The development of affordable and energy-efficient materials for the chemical and petrochemical industry is crucial as this sector is the largest consumer of energy and the third largest direct emitter of greenhouse gases.[1,2] The demand for new materials for CO_2 capture or separation from natural gas is of significant importance. New effective sorbents are expected to meet many important criteria such as high capacity, selectivity and stability, as well as recyclability and fast kinetics.[3,4] Small-pore zeolites are attractive candidates because of the shape and size and of the pores, as well as the presence of extra-framework cations.[5] By blocking the pore entries, the extra-framework cations selectively provide access for molecules to the zeolite channels and cages depending on the nature of the molecules.[6] A high selectivity towards CO_2 over CH_4 for small-pore zeolites with RHO, MER and CHA type framework has been observed, indicating that the cation gating effect permits the uptake of CO_2 but not CH_4.[7,8]

The framework of CHA type zeolites consists of double 6-membered ring (D6R) and *cha* cage units, where the super cages (10 × 8 × 8 $Å^3$) are interconnected by a 3-dimensional pore system with 8-membered ring (8MR) entries (3.8 × 3.8 $Å^2$). [9] The selective adsorption of CO_2 in CHA zeolites containing various cations (K^+, Rb^+, or Cs^+) have been investigated demonstrating that the cations controlling the adsorption of CO_2 over CH_4 are the ones located at the centre of the 8MRs. Their high separation ability was attributed to cation gating behaviour described as a molecular "trapdoor" mechanism.[10-13] Shang *et al.* [6] proposed that CO_2 and CO interact strongly with the 8MR door-keeping cations (K^+, Rb^+, Cs^+) due to their respective quadrupole and dipole moment and higher polarizability as compared to N_2 and CH_4. This interaction displaces the door-keeping cations located at site SIII' (**Figure 1a**) from the 8MR, allowing the selective entry of molecules into the super cage of the CHA zeolite. The cation displacement is temporary and reversible, thus the "weakly" interacting molecules such as CH_4 and N_2 are excluded while CO and CO_2 are selectively adsorbed. Shang *et al.* [11] determined that a CHA zeolite with an Si/Al ratio lower than 3 will display "trapdoor" behaviour for the selective CO_2 adsorption from a mixture containing CH_4 provided the extra-framework cations are located at the centre of the 8MRs.

So far, CHA type zeolites have been synthesised using organic structure-directing agents (OSDAs),[14] seeds[15] or by recrystallization of H-FAU zeolite to K-CHA under alkaline treatment.[16] Previously, Liu *et al.*[17] reported the synthesis of OSDA-free pure CHA-type zeolite using NH_4F. This method affords micron-sized crystals of 15–20 µm with a low amount of defects, however, the large size of the crystals affects their performance in gas adsorption[18] and catalysis[19] due to diffusion limitations. Up to now, nanosized CHA zeolite has been obtained either by recrystallization of FAU-type zeolite synthesized with the assistance of an OSDA[20] or by ball milling.[21] We here report on the OSDA-free synthesis of a CHA type zeolite with excellent CO_2 sorption capacity and selectivity.

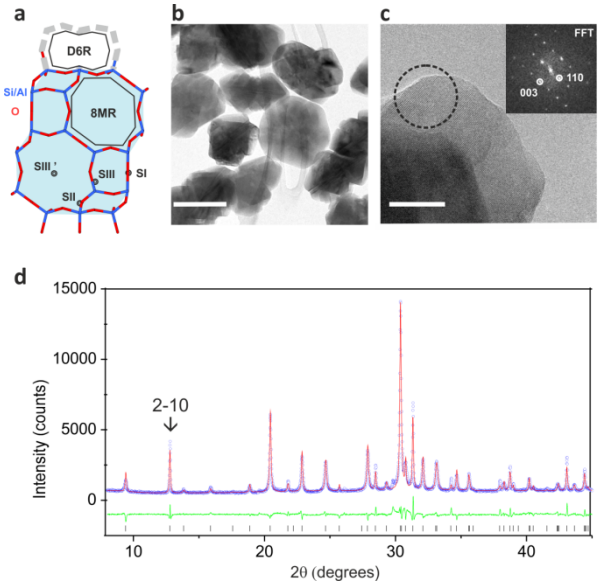

Figure 1. Identification of nanosized CHA. a, CHA framework (SG: *R*-3*m*) projected along the *b*-axis showing the super cage (in light blue). Bonds between Si/Al (tetrahedral sites) and oxygens, D6R and 8MR units and sites for extra-framework cations (denoted S) are indicated for clarity. **b**, TEM image of nanosized CHA crystals synthesized without OSDAs in aqueous solution under hydrothermal synthesis conditions (90 °C for 8 h). Length of the scale bar is 200 nm. **c**, High-resolution TEM image of a crystallite looking along [1-10]. Length of the scale bar is 40 nm. Inset: Fourier transform from the area encircled in black. **d**, Le Bail refinement of the powder X-ray diffraction pattern of the as-synthesized CHA nanosized crystals.

Nanosized CHA type zeolite crystals with a size below 200 nm and a Si/Al ratio of 2.0 are obtained by direct hydrothermal treatment of colloidal precursor suspensions containing a mixture of inorganic structure directing cations only (Na^+, K^+ and Cs^+). The nanosized CHA crystals with plate-like morphology are shown in **Figure 1b and c**. The mixed inorganic cations were not only used to prepare the clear colloidal precursor suspensions, but also to prevent Ostwald ripening[22] during the crystallization process and facilitate the formation of nanosized CHA crystals. The use of the mixture of three inorganic cations (Na^+, K^+ and Cs^+) is required, and their concentration was fine-tuned in order to synthesize nanosized CHA zeolite crystals free of impurities (**Figure 1d, Table S1**). The formation of secondary phases, such as RHO or FAU type zeolites, was avoided by optimizing the chemical composition of the colloidal precursor suspensions and the physical parameters controlling the synthesis (time of aging, speed of stirring, and synthesis temperature) (**Table S1**). The Le Bail refinement of the powder X-ray diffraction (PXRD) pattern (**Figure 1d**) using the space group *R*-3*m* confirmed that single phase CHA zeolite was synthesized. The refinement also revealed the presence of anisotropic peak broadening due to the plate-like shape of the crystallites and a certain degree of structural disorder. The size of the CHA crystallites, as estimated by the Scherrer equation,[23] is approximately 42 nm (thickness, along the *c*-axis) by 189 nm (width, in the *ab*-plane) which is in agreement with the HRTEM observations. Furthermore, the NMR spectroscopic results confirmed the formation of crystalline CHA zeolite. The ^{27}Al NMR spectrum contains only one peak at 57.8 ppm corresponding to tetrahedrally coordinated Al (**Figure S1**), while the ^{29}Si NMR spectrum contains peaks at -89.3 ppm, -93.6 ppm, -99.1 ppm, -104.6 ppm and -109.1 ppm corresponding to Q^0 (4Al), Q^1 (3Al), Q^2 (2Al), Q^3 (1Al) and Q^4 (0Al) silicon tetrahedrally coordinated, respectively.[24] A Si/Al ratio of 2.0 was estimated according to the equation of Engelhardt and Michel using the ^{29}Si NMR data.[25]

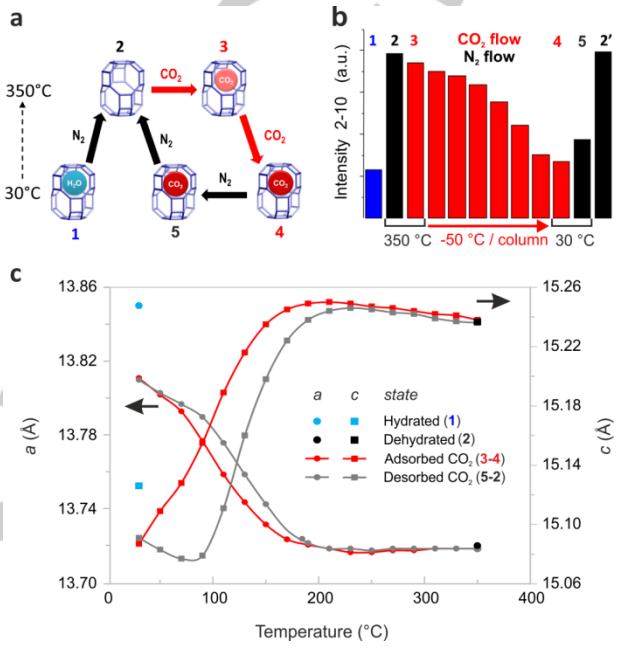

Figure 2. *In-situ* PXRD study. CHA nanocrystals were subjected to adsorption of CO_2 after activation (350 °C under N_2): (**a**) schematic representation of the measurement cycles at different temperatures and atmospheres. The as-synthesized CHA was activated under heating at 350 °C (Steps 1 to 2). Then the samples were measured at 350 °C under CO_2 flow (40 mL.min^{-1} keeping the pressure at 1 bar) with decreasing the temperature until room temperature (Steps 3 to 4). The CHA was reactivated under heating at 350 °C to desorb the CO_2 molecules (Steps 5 to 2'). More details are provided in the experimental section (method). **b**, Change of the diffraction intensity of 2-10 reflection at 12.8° (2θ) over the measurement cycle. **c**, Evolution of the unit-cell parameters *a* (disks) and *c* (squares) vs temperature and atmospheres.

The mechanism of selective CO_2 adsorption by OSDA-free nanosized CHA zeolite was investigated by several complementary *in situ* methods. Initially, the changes to the crystallographic properties of the nanosized CHA crystals under adsorption of CO_2 were studied by *in situ* PXRD. The measurements were performed following a protocol schematically presented in **Figure 2a**. The nanosized CHA zeolite was activated in the *in situ* cell under N_2 atmosphere (1 bar) at 350 °C, then CO_2 (1 bar) was delivered under gradual decrease of the temperature from 350 °C to room temperature (RT). Dehydration of the as-prepared CHA, was confirmed by an increase of the intensity of the Bragg peak at 12.8° 2*θ* corresponding to the 2-10 reflection (**Figure 2b**), a decrease of the *a* lattice parameter and an increase of the *c* lattice parameter (**Figure 2c**). These parameters are sensitive to the presence of adsorbed molecules and can be used to monitor

CO_2 adsorption as a function of temperature. As shown in **Figure 2c**, the adsorption of CO_2 begins to occur at approximately 200 °C. This agrees well with the thermogravimetric analyses (TGA) carried out following the same protocol (**Figure 3a**). Based on the TGA, the number of CO_2 and H_2O molecules per unit cell was estimated to be 8 and 28 for CO_2-loaded and hydrated nanosized CHA zeolite sample, respectively (**Table S2**). In addition, TGA (**Figure 3a**) over 10 cycles of CO_2 adsorption/desorption show that the sorption capacity of the nanosized CHA zeolite is fully preserved. The high stability and regenerability of the nanosized CHA zeolite is also confirmed by the absence of any changes in the PXRD patterns of the sample after 10 cycles (**Figure S2**). The nanosized CHA zeolite adsorbed 3.8 mmol/g CO_2 at 121 kPa and 273 K (**Figure S3**) which is significantly higher than the Cs-CHA prepared by ion exchange from OSDA synthetized CHA (< 2.5 mmol/g at 253 K)[6] and similar to the pure K-CHA zeolite (> 4 mmol/g). This value is also comparable with the maximum CO_2 uptake obtained in SSZ-13 (CHA type) zeolites.[26,27] After demonstrating the high CO_2 adsorption capacity of the nanosized CHA type zeolite, the selectivity was investigated by studying the adsorption of CH_4. The nanosized CHA zeolite demonstrated high selectivity for CO_2 over CH_4 as shown by both TGA (**Figure 3**) and *in situ* FTIR (**Figure S4**) experiments. The selective CO_2 adsorption in the CHA zeolite is confirmed by the presence of a band at 2345 cm^{-1} corresponding to the physisorbed CO_2, and bands in the range 1316–1680 cm^{-1} representing the chemisorbed CO_2 (**Figure S4a**). No CH bands in the region 2700–2900 cm^{-1} corresponding to CH_4 are present in the IR spectra (**Figure S4b**). In terms of the CO_2 adsorption capacity and selectivity, the performance of the nanosized CHA rivals the best CHA zeolites synthesized using OSDA.[26-27] This goal is reached without the need for high-temperature calcination (above 500 ºC) to eliminate the OSDA and post-synthetic ion exchange to ensure CO_2 selectivity.

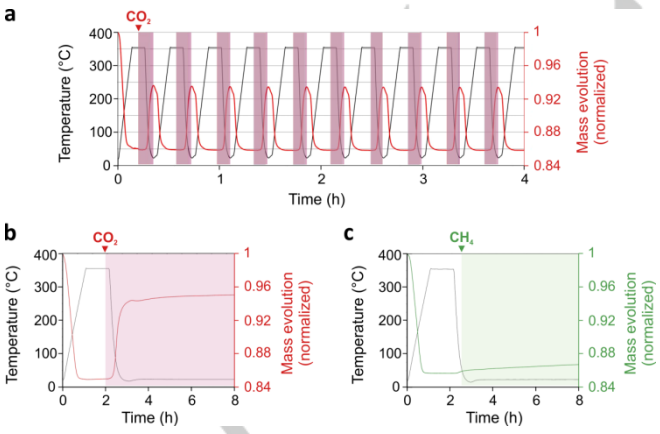

Figure 3. CO_2 vs CH_4 absorption. a, Thermogravimetric analysis (TGA) of nanosized CHA zeolite subjected to 10 consecutive adsorption/desorption cycles of CO_2: temperature variation (black line), CO_2 sorption (red rectangles) and mass variation (red line). **b**, mass variation upon CO_2 adsorption (red line) and (**c**) CH_4 adsorption (green line) on as-synthesized nanosized CHA. The CH_4 flow was delayed and started at 25 °C instead of 350 °C for safety reasons.

To gain further insight into the selective CO_2 adsorption by the nanosized CHA, a single crystal structure investigation was performed on a CO_2 loaded sample in order to obtain a complete structure determination including the localization of extra-framework cations and guest molecules (CO_2). In the past, the fine structure of Chabazite was investigated by single crystal X-ray diffraction.[28] In our case, due to the small size of the CHA nanocrystals (less than 10^{-2} μm^3), structure analysis based on precession-assisted 3D ED[29] was carried out. The measurements of six different nanosized single crystals were combined to obtain a high-quality data set (**Table S3**). The electrostatic potential map obtained by *ab initio* structure solution (charge flipping method[30]) revealed two occupied extra-framework sites: Site SII above the D6R with oxygen distances of about 2.8 Å and Site SIII' at the center of the 8MR with oxygen distances between 3.2 and 3.5 Å (**Figure 4**). Taking dynamical diffraction effects into account,[31] a structural model for the nanosized CHA zeolite was refined with an overall composition of $Cs_{6.61(2)}K_{3.6}Na_{2.4}(Si_{23.4}Al_{12.6})O_{72}(CO_2)_8$, which is in agreement with the chemical composition $Cs_{6.3(4)}K_{3.6(2)}Na_{2.5(5)}(Si_{23.6(9)}Al_{12.4(7)})O_{72}(CO_2)_{8.0(3)}$ determined by EDX combined with TGA.

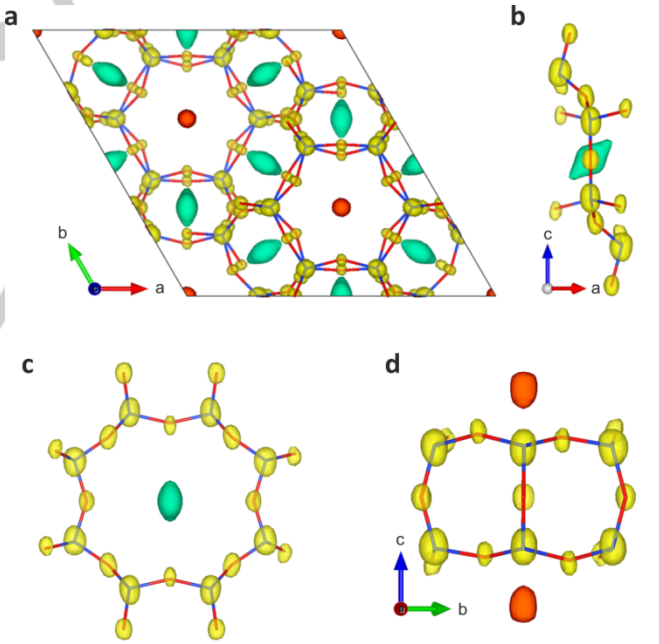

Figure 4. Structure solution. Electrostatic potential map obtained from *ab initio* structure solution using single nanocrystals PEDT datasets. Isosurface levels correspond to 3.5σ[V(r)]. **a**, Projection along *c*. Yellow, red and green transparent colours indicate framework, SII and SIII' sites, respectively. Tetrahedral sites (blue lines) and framework oxygen atoms (red lines) are included for clarity. **b**, Side view of eight membered ring (8MR) with elongated potential around SIII' site. **c**, Perpendicular view of 8MR. **d**, Side view of D6R with SII sites.

The refinement results (more details in Supporting Information) indicate that the SII site is a split site occupied by Na (40%) and K (60%), whereas the SIII' site is partially occupied by 73.4(3)% Cs only (**Table S4** and **Figure S5**). Despite having less than 1 Cs^+ cation per 8MR, this CHA zeolite exhibits an overall molecular "trapdoor" effect that prevents CH_4 to be adsorbed. [11] A remarkable feature illustrating the role of the Cs^+ cation in the "trapdoor" effect is that the mean atomic displacement parameter of the Cs^+ cation perpendicular to the 8MR door is very large ($U_\perp$ = 0.346 Å²) compared to the displacements parallel to the 8MR ($U_\parallel$ = 0.019 and 0.030 Å²). Cs^+ cations are strongly displaced back and forth from the center of the 8MR site even at low temperature (T = 100 K). This is consistent with previous NMR measurements and DFT calculations on Cs-exchanged CHA where the Cs^+ cations were reported to demonstrate greater mobility in the presence of CO_2.[6] The possibility to have such an atomic displacement induced by the electron beam can be disregarded as similar behavior is confirmed from Rietveld refinement based on the PXRD data recorded at room temperature (see Supporting Information). This tendency of the door-keeping cation to move away from its average position allows some molecules to go through and enter the supercage. After the completion and refinement of the host structure, the difference potential map revealed the position of the CO_2 guest molecules within the *cha* supercage (**Figure 5**). Even though the individual atoms were not well discernible, the position of the CO_2 molecule refined to reasonable values, and the refinement was stable with a minimum set of constraints on the molecule geometry (**Tables S5** and **S6**). The CO_2 molecules are approximately aligned with the long axis of the CHA unit cell and coordinate the extra-framework cations. The shortest host-guest contacts are 2.621(12) Å for CO_2–K^+ and 3.105(9) Å for CO_2–Cs^+ (**Table S7**). This is, to our knowledge, the first direct determination of the CO_2 position in CHA zeolite with low Si/Al ratio. Notably, this position is different from any of the positions found in Li-, Na- and K-CHA zeolites using neutron powder diffraction data[9], where CO_2 is located predominantly in the center of the 8MR at site SIII'. Noteworthy, the refined CO_2 position, the CO_2–Cs^+ distance and the increased mobility of Cs due to the presence of guest CO_2 are consistent with first principle calculations performed for low Si/Al ratio Cs-CHA zeolites.[32] The position of the CO_2 molecules was also confirmed by Rietveld refinement of PXRD data (**Tables S8-S9** and **Figure S8**), complementing the ED results. These structural results are further supported by the superposition of the calculated micropore volume of the *cha* cage and the refined position of the CO_2 molecule (**Figure 5**).

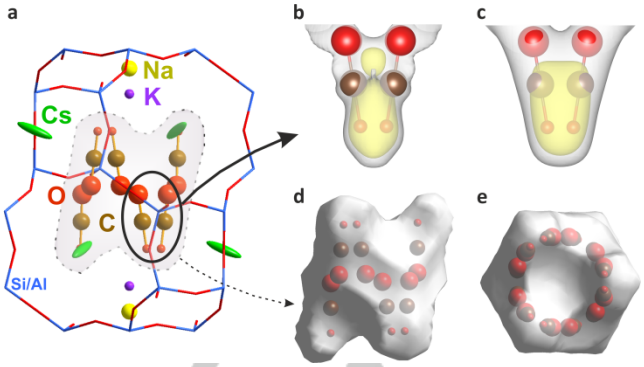

Figure 5. CO_2 position in nanosized CHA zeolite probed by electron diffraction. a, Projection of the refined structure along the *a* direction showing the localization of CO_2 molecules inside the super cage. The plotted atom size represents a probability sphere of 40% for the extra-framework cations and 10% for the CO_2 molecules based on refined ADPs. **b**, Overlay of difference potential map (grey and yellow isosurface levels correspond to 2σ[ΔV(r)] and 3σ[ΔV(r)], respectively) and the refined position of the CO_2 molecule. **c**, Expected potential map based on calculated structure factors. In (**d**) and (**e**), the positions of the CO_2 molecules are superimposed on the void volume of the *cha* cage along *a* and *c* direction, respectively. The occupancy of each displayed CO_2 molecule is 22.2%, i.e. on average only 2.67 of the 12 shown molecule sites are occupied.

Eight CO_2 molecules per unit cell correspond to ~2.5 mmol/g, which is less than the measured sorption capacity at ambient pressure (**Figure S3**). We identified a similar discrepancy between the crystallographic results and sorption measurements in the work by *Pham et al.*[27] A likely explanation is that crystallographic studies are only sensitive to CO_2 molecules that are adsorbed inside the zeolite crystals, *i.e.* in the cages. However, CO_2 is adsorbed in the mesopores between the CHA nanocrystals (textural mesopores) and at the surface of the crystals that increases the amount of the measured CO_2. From single crystal diffraction data,[33] the estimated volume needed by a single CO_2 molecule in a solid is ~44.5 Å^3. Considering the CHA framework and extra-framework cations, the volume accessible to CO_2 molecules is approximately 500 Å^3 per unit cell, which corresponds to a maximum of about 11 CO_2 molecules per unit cell. About 73% of this hypothetical upper limit is reached in our nanosized CHA zeolite sample. Taking inter-atomic distances into account, any so far reported CO_2 site in CHA[27] does not allow to host more than 9 molecules per unit cell (see Supporting Information). This limit is obeyed in CHA zeolites with Si/Al = 6–12 reported by *Pham et al.*[27] The refined number of molecules is ~8.2 for both Li- and Na-CHA, ~5.5 for pure Si-CHA (all three based on powder neutron diffraction at T = 10 K) and ~6.0 for K-CHA (based on PXRD). However, the majority of the molecules in all these zeolites occupies the 8MR, rendering the desirable trapdoor effect impossible. Thus, with 8 CO_2 per unit cell, the CHA zeolite of this work reaches an almost perfect CO_2 storage capacity together with the excellent selectivity (no CH_4 was adsorbed).

In summary, we report the direct and environmentally benign synthesis of nanosized CHA zeolite (Si/Al = 2) without the use of OSDAs. A mixture of three alkali cations, Cs^+, K^+ and Na^+, was used as an inorganic templating agent to direct the synthesis of the

nanosized CHA zeolites, and in particular Cs^+ was employed as the primary cation responsible for the selective adsorption of CO_2 over CH_4. In addition to the improvement in the pore accessibility and the adsorption kinetics, the nanosized CHA zeolite demonstrated a high CO_2 absorption capacity. Moreover, the Cs^+ cations improve the stability of the CHA structure, demonstrating recyclability under high temperature treatment and multi-cycle CO_2 adsorption experiments. This environmentally benign synthesis of CHA nanocrystals is energy-efficient and more affordable than other methods reported so far in the open literature. Potentially scalable for industrial applications, the nanosized CHA zeolite is a highly promising material for applications in both CO_2 capture and CO_2/CH_4 separation.

Acknowledgements

Financial support from CARNOT ESP (project NZAMS-CO2), TOTAL and Industrial Chair ANR-TOTAL "Nanoclean Energy" is acknowledged, as well as from the Normandy Region through the RIN Recherche Program. The work at IoP Prague was performed withing CzechNanoLab Research Infrastructure supported by MEYS CR (LM2018110) using instruments of the ASTRA laboratory established within the Operation program Prague Competitiveness project CZ.2.16/3.1.00/24510 and supported by the Czech Science Foundation, project number 19-08032S.

Keywords: Nanozeolites • Template-free synthesis • CO_2 adsorption • CO_2 In-situ PXRD • precession-assisted 3D ED.

[1] M. Fischedick, J.Roy, Climate Change 2014: Mitigation of Climate Change, in Chapter 10 - Industry. IPCC Working Group III Contribution to AR5 (Cambridge University Press, **2014**).
[2] Tracking Clean Energy Progress. https://www.iea.org/topics/tracking-clean-energy-progress.
[3] H. A. Patel, J. Byun, C. T. Yavuz, Carbon Dioxide Capture Adsorbents: Chemistry and Methods. *ChemSusChem,* **2017**, 10,1303 –1317
[4] M.C. Bacariza, I. Graça, J.M. Lopes, C. Henriques. Tuning Zeolite Properties towards CO2 Methanation: An Overview. *ChemCatChem*, **2019**, 11, 2388–2400.
[5] M. Dusselier, and M.E. Davis, Small-Pore Zeolites: Synthesis and Catalysis. *Chem. Rev.* **2018**,118, 5265–5329.
[6] J. Li. Shang, R. Singh, Q. Gu, K. M. Nairn, T. J. Bastow, N. Medhekar, C. M. Doherty, A. J. Hill, J. Z. Liu, P. A. Webley, Discriminative separation of gases by a 'molecular trapdoor' mechanism in chabazite zeolites. *J. Am. Chem. Soc.*, **2012**, 134, 19246–19253.
[7] V. M. Georgieva, L. E. Bruce, M.C. Verbraeken, A. R. Scott, W. J. Casteel, Jr. S. Brandani, P.A. Wright, Triggered Gate Opening and Breathing Effects during Selective CO_2 Adsorption by Merlinoite Zeolite. *J. Am. Chem. Soc.* **2019**, 141, 12744–12759.
[8] M. Palomino, A. Corma, J. L. Jordá, F. Rey, S. Valencia, Zeolite Rho: a highly selective adsorbent for CO_2 /CH_4 separation induced by a structural phase modification. *Chem. Commun.* **2012**, 48, 215–217.
[9] L. Smith, H. Eckert, A. K. Cheetham, Site Preferences in the Mixed Cation Zeolite, Li,Na-Chabazite: A Combined Solid-State NMR and Neutron Diffraction Study. *J. Am. Chem. Soc.* **2000**, 122, 1700–1708.
[10] T. Du, X. Fang, L. Liu, J. Shang, B. Zhang, Y. Wei, H. Gong, S. Rahman, E. F. May, P. A. Webley, G. Li, An optimal trapdoor zeolite for exclusive admission of CO_2 at industrial carbon capture operating temperatures. *Chem. Commun.* **2018**, 54, 3134–3137.
[11] J. Shang, G. Li, R. Singh, P. Xiao, J. Z. Liu, P. A. Webley, Determination of Composition Range for "Molecular Trapdoor" Effect in Chabazite Zeolite. *J. Phys. Chem. C,* **2013**, 117, 12841–12847.
[12] J. Shang, G. Li, R. Singh, P, Xiao, D. Danaci, J. Z. Liu, P. A. Webley, Adsorption of CO_2, N_2, and CH_4 in Cs-exchanged chabazite: A combination of van der Waals density functional theory calculations and experiment study. *J. Chem. Phys.* **2014**, 140, 084705.
[13] G. Li, J. Shang, Q. Gu, R. V. Awati, N. Jensen, A. Grant, X. Zhang, D. S. Sholl, J. Z. Liu, and P. A. Webley, E.F. May, Temperature-regulated guest admission and release in microporous materials. *Nat. Commun.* **2017**, 8.
[14] S. I. Zones, Zeolite SSZ-13 and its method of preparation. US Patent 4, **1985**, 544,538.
[15] H. Imai, N. Hayashida, T. Yokoi, T. Tatsumi, Direct crystallization of CHA-type zeolite from amorphous aluminosilicate gel by seed-assisted method in the absence of organic-structure-directing agents. *Microporous and Mesoporous Mater.* **2014**, 196, 341–348.
[16] M. Bourgogue, J-L. Guth, R. Wey, Process for the preparation of synthetic zeolites, and zeolites obtained by this process. US Pat. **1985**, 4503024. 10.
[17] B. Liu, Y. Zheng, N. Hu, T. Gui, Y. Li, F. Zhang, R. Zhou, X. Chen, H. Kita, Synthesis of low-silica CHA zeolite chabazite in fluoride media without organic structural directing agents and zeolites. *Microporous Mesoporous Mater.* **2014**, 196, 270–276.
[18] S. Prodinger, R. S. Vermuri, T. Varga, B. P. McGrail, R. Kishan, M. A. Derewinski, Impact of chabazite SSZ-13 textural properties and chemical composition on CO_2 adsorption applications. *New J. Chem.* **2016**, 40, 4375–4385.
[19] Z. Li, M.T. Navarro, J. Martínez-Triguero, J. Yu, A. Corma, Synthesis of nano-SSZ-13 and its application in the reaction of methanol to olefins. *Catal. Sci. Technol.* **2016**, 6, 5856–5863.
[20] T. Takata, N. Tsunoji, Y. Takamitsu, M. Sadakane, T. Sano, Nanosized CHA zeolites with high thermal and hydrothermal stability derived from the hydrothermal conversion of FAU zeolite. *Microporous Mesoporous Mater.* **2016**, 225, 524–533.
[21] C. Anand, T. Kaneda, S. Inagaki, S. Okamura, H. Sakurai, K. Sodeyama, T. Matsumoto, Y. Kubota, T. Okubo, T. Wakihara. Downsizing the K-CHA zeolite by a postmilling-recrystallization method for enhanced base-catalytic performance. *New J. Chem.* **2016**, 40, 492–496.
[22] S. Mintova, J.-P. Gilson, V. Valtchev, Nanoscale **2013**, 5, 6693-6703
[23] A. L. Patterson, The Scherrer Formula for X-Ray Particle Size Determination. *Phys. Rev.* **1939**, 56, 978–982.
[24] G. T. M. Kadja, I. R. Kadir, A. T. N. Fajar, V. Suendo, R. R. Mukti, Revisiting the seed-assisted synthesis of zeolites without organic structure-directing agents: insights from the CHA case. *RSC Adv.* **2020**, 10, 5304-5315,
[25] G. Engelhardt, D. Michel, in "High-Resolution Solid-State NMR of Silicates and Zeolites"*, Wiley & Sons*, New York, **1987**.
[26] M.R. Hudson, W.L. Queen, J.A. Mason, D.W. Fickel, R.F. Lobo, C.M. Brown, Unconventional, highly selective CO_2 adsorption in zeolite SSZ-13. *J. Am. Chem. Soc.* **2012**, 134, 1970–1973.
[27] T. D. Pham, M. R. Hudson, C. M. Brown, R. F. Lobo, Molecular Basis for the High CO_2 Adsorption Capacity of Chabazite Zeolites. *ChemSusChem*, **2014**, 7, 3031–3038.
[28] L.S. Dent, J.V. Smith, Crystal structure of chabazite, a molecular sieve. *Nature,* **1958**, 181, 1794-1796.
[29] M. Gemmi, E. Mugnaioli, T. E. Gorelik, U. Kolb, L. Palatinus, P. Boullay, S. Hovmöller. J. P. Abrahams, 3D Electron Diffraction: The Nanocrystallography Revolution. *ACS Cent. Sci.* **2019**, 5, 1315–1329.
[30] L. Palatinus, G. Chapuis, Superflip - a computer program for the solution of crystal structures by charge flipping in arbitrary dimensions. *J. Appl. Cryst.* **2007**, 40, 786-790.
[31] L. Palatinus, C. A. Corrêa, G. Steciuk. D. Jacob, P. Roussel, P. Boullay, M. Klementová, M, Gemmi, J, Kopeček. M. C. Domeneghetti, F. Cámara, V. Petříček, Structure refinement using precession electron diffraction tomography and dynamical diffraction: tests on experimental data. *Acta Cryst.* **2015**, B71, 740–751.
[32] J. Shang, G. Li, P.A. Webley, J.Z. Liu. A density functional theory study for the adsorption of various gases on a caesium-exchanged trapdoor chabazite. *Comput. Mater. Sci.* **2016**, 122, 307–313.
[33] A. Simon, K. Peters, Single-Crystal Refinement of the Structure of Carbon Dioxide, *Acta Crystallogr.*, **1980**, B36, 2750-2751.

Entry for the Table of Contents

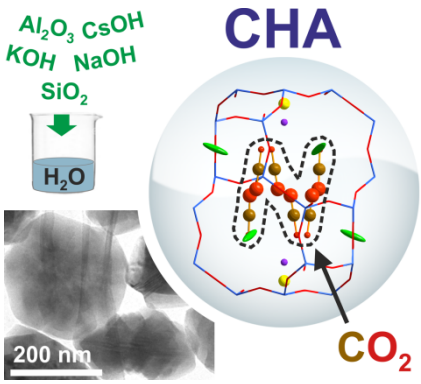

We report on the synthesis of nanosized CHA type zeolite without organic structure-directing agents. The zeolite material exhibits excellent CO_2 storage capacity, a high stability under high temperature treatment and selectivity towards CO_2 over CH_4, controlled by Cs+ in the host structure. The environmentally benign and energy-efficient synthesis of CHA nanocrystals is more affordable than other methods reported so far in the open literature.